Supporting Information

Marlow et al. 10.1073/pnas.1001896107

SI Materials and Methods

Transplant Techniques. To generate chimeric mammary glands with *Slit2*$^{-/-}$;*Slit3*$^{-/-}$ epithelium in a $^{+/+}$ host background mammary anlage were rescued from E16-20 embryos and transplanted into precleared fat pads of athymic nude (*Foxn1*^{nu}), 3-wk-old mice (1). After 10–12 wk, epithelial tissue fragments were contralaterally transplanted to generate knockout and wild-type tissue (2). To generate chimeric mammary outgrowths in host *Robo4*$^{-/-}$ stroma, adult (10- to 12-week-old) epithelial fragments from WT and *Robo1*$^{-/-}$ donor mice were harvested and contralaterally transplanted into precleared fat pads of syngeneic *Robo4*$^{-/-}$ host mice.

Antibodies. The following antibodies were used: anti-CK-14 (Covance), anti-PECAM (BD Biosciences), anti-ROBO1 (Abcam), anti-SDF-1 (Santa Cruz Biotechnology), anti-SLIT2 (Abcam), anti-SLIT3 (Chemicon), anti-SMA (1A4; Sigma), anti-PY397-FAK (Invitrogen), anti-Src (Cell Signaling), anti-PY416-Src (Cell Signaling), anti-VEGF-A (Santa Cruz Biotechnology), anti-VEGFR2 (Cell Signaling), anti-PY1175-VEGFR2 (Cell Signaling), anti-phosphotyrosine (4G10; Millipore), Alexa Fluor 555 donkey anti-goat, Alexa Fluor 555 donkey anti-mouse, Alexa Fluor 488 and 568 goat anti-rabbit, Alexa Fluor 488 and 555 goat anti-rat (Invitrogen).

Immunohistochemistry. Standard protocols were used (2). For paraffin embedding, tissue was fixed in 4% PFA, embedded and sectioned at 7–10 μm. Frozen tissue was embedded in O.C.T Compound (Tissue Tek) and sectioned at 10–30 μm using a Leica CM3050S Cryostat. For visualization of nuclei, either DAPI or hematoxylin nuclear counter stains were used. Secondary antibodies were either fluorescently conjugated or conjugated to HRP for visualization with DAB (3,3-Diaminobenzidine). *Robo1* expression was assessed using beta-galactosidase activity on frozen sections (25 μm). Following X-Gal treatment, slides were fixed and counterstained. Immunostaining was scored according to percentage positive cells (P) and staining intensity (I). Score equals P+I. (*P* scores 0 (none), 1 (<1%), 2 (1–10%), 3 (10–30%), 4 (30–60%), 5 (>60%). I scores 0 (none), 1 (weak), 2 (intermediate), 3 (strong).

Microscopy, Image Acquisition, and Processing. For brightfield and fluorescent microscopy, images were captured on a Zeiss Axiovert 200 microscope. Confocal microscopy was performed using a Zeiss LSM 5 Pascal confocal microscope. Confocal images, taken as Z-stacks, were compressed as Sum intensity and saved as JPEGs using the LSM Reader plug-in for ImageJ (National Institutes of Health).

Blood Vessel Density, Branchpoints, and Tortuosity. For evaluation of blood vessel density, 30-μm tissue sections were chosen at intervals of 120 μm and probed with anti-PECAM antibody (Invitrogen). The same excitation, gain and exposure settings were applied for each slide. Processed images were imported to ImageJ where intensity threshold was set automatically and analyzed for units of positive pixel area with a minimum threshold of 50 μm^2. Results were displayed as Area Fraction + (Positive Pixel Area/Total Area × 100). For analysis of blood vessel density in virgin glands, slides were masked to prevent bias and imaged at 20× magnification. No less than three FOV were obtained per section, no less than 10–15 FOV were obtained per animal and no less than three animals were evaluated. At pregnancy day 12.5, stromal and epithelial-bound blood vessels exist in approximately equal numbers, to analyze blood vessel density the above methodology was applied. Branch points were counted using ImageJ. For tortuosity, a total of three blood vessels were measured per image (ImageJ) and expressed as a quotient: length of blood vessel over distance between ends.

Primary Cell Culture. Primary mammary epithelial cells were isolated using mild collagenase and dispase digestion. Cells were cultured on plastic for 2 days, then serum-starved for 2 h and treated for 24 h with 200 μg/mL SDF1 (Peprotech).

RNA Extraction and RT-PCR. RNA was extracted from primary cells using PureLink RNA Mini Kit (Invitrogen). RT-PCR was performed using iScript cDNA Synthesis Kit (Bio-Rad). Primers for *Vegf-A* and *GAPDH* were used (3).

Endothelial Cell Migration. Equimolar hu*Robo1* siRNA (Hs_Robo1_11_HP; Qiagen), hu*Robo4* siRNA (Hs_Robo4_1_HP; Qiagen) or AllStars Negative Control siRNA (Qiagen) transfection complexes were formed according to standard protocol and added to Human MicroVascular Endothelial Cells-Lung (HMVEC-L; Lonza). Companion dishes were proportionally prepared to assess knockdown of gene expression. Forty-eight hours later, cells were serum starved and 30,000 cells were seeded per fibronectin coated 8 μm 6.5-mm transwell (Costar). Cells were allowed to migrate to 2 nM VEGF in the presence of 10 nM Slit2N or Mock for 20 h. Filters were removed, migrated cells were counterstained, and eight high power fields per filter were counted. Fold migration over unstimulated were determined and data are presented as mean ± SEM of at least three independent experiments performed in at least triplicate.

Immunoprecipitation and Immunoblotting. Mammary glands were lysed in RIPA buffer; 500 mg of lysate was used for immunoprecipitation of VEGFR2 (4). Immunoblotting was performed as previously described (2). Equal total protein was loaded (20 μg/lane) and checked using a reference protein. Blots were scanned at 300 dpi and band intensities were calculated using ImageJ. For each experimental set, at least three replicate samples were probed and average band intensity calculated. For statistical analysis, sample values were normalized to that of average wild-type band intensity.

Statistical Analysis. We used factorial design ANOVA or unpaired *t* tests to analyze data as appropriate. Significant ANOVA values were subjected to posttest using the Tukey-Kramer comparison. We report *P* values for each statistical test. Data not significantly different had $P > 0.05$.

1. Robinson GW, Accili D, Hennighausen L (2000) *Rescue of Mammary Epithelium of Early Lethal Phenotypes by Embryonic Mammary Gland Transplantation as Exemplified with Insulin Receptor Null Mice* (Kluwer Academic/Plenum Press, New York), pp 307–316.
2. Marlow R, et al. (2008) SLITs suppress tumor growth in vivo by silencing Sdf1/Cxcr4 within breast epithelium. *Cancer Res* 68:7819–7827.
3. Hovey RC, Goldhar AS, Baffi J, Vonderhaar BK (2001) Transcriptional regulation of vascular endothelial growth factor expression in epithelial and stromal cells during mouse mammary gland development. *Mol Endocrinol* 15:819–831.
4. Stockmann C, et al. (2008) Deletion of vascular endothelial growth factor in myeloid cells accelerates tumorigenesis. *Nature* 456:814–818.

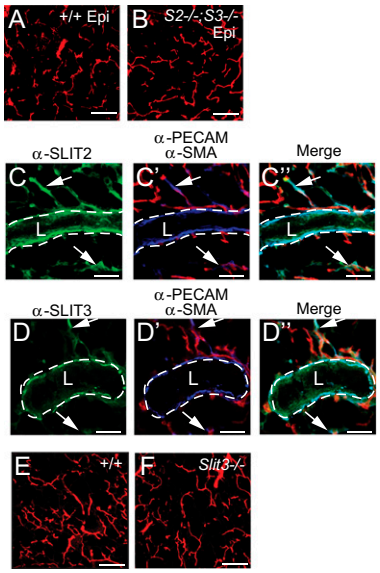

Fig. S1. SLIT2 and SLIT3 are expressed in the mammary gland, but loss of their expression does not enhance blood vessel growth. (*A* and *B*) Lack of *Slit* in the epithelium does not alter blood vessel density in outgrowths. Representative images of $^{+/+}$ (*A*) and *Slit3*$^{-/-}$ (*B*) mammary sections immunostained with anti-PECAM (red). (Scale bar, 50 μm.) (*C and D*) SLIT2 and SLIT3 are expressed in both the epithelial and stromal compartments of the mammary gland. Representative immunostaining of anti-SLIT2 (green) (*C*), anti-PECAM (red) (*C′*), and anti-SMA (blue) (*C″*) on mammary sections. Arrows indicate mural cell localization. Dashed line denotes the boundary of the epithelium. L = Lumen. (Scale bar: 50 μm.) Representative immunostaining of anti-SLIT3 (green) (*D*), anti-PECAM (red) (*D′*), and anti-SMA (blue) (*D″*) on mammary sections. Arrows indicate mural cell localization. Dotted line denotes the boundary of the epithelium. L, lumen. (Scale bar, 50 μm.) (*E* and *F*) Lack of *Slit3* does not increase blood vessel number in the mammary gland. Representative images of $^{+/+}$ (*E*) and *Slit3*$^{-/-}$ (*F*) mammary sections immunostained with anti-PECAM (red). (Scale bar, 50 μm.)

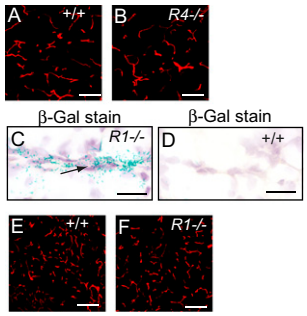

Fig. S2. Loss of either Robo4 or Robo1 does not enhance blood vessel growth. (*A* and *B*) Lack of *Robo4* does not alter blood vessel density in the mammary gland. Representative images of $^{+/+}$ (*A*) and *Robo4*$^{-/-}$ (*B*) sections immunostained with anti-PECAM (red). (Scale bar, 50 μm.) (*C* and *D*) ROBO1 is expressed by blood vessels. Representative images of *Robo1* by β-galactosidase activity on *Robo1*$^{-/-}$ tissue that contains *LacZ* inserted under the control of the *Robo1* promoter (turquoise) (*C*). No staining is observed in $^{+/+}$ tissue (*D*). Arrow indicates positive cells in the endothelium. (Scale bar, 20 μm.) (*E* and *F*) Lack of *Robo1* does not alter blood vessel density in the mammary gland. Representative images of $^{+/+}$ (*E*) and *Robo1*$^{-/-}$ (*F*) mammary sections immunostained with anti-PECAM (red). (Scale bar, 50 μm.)

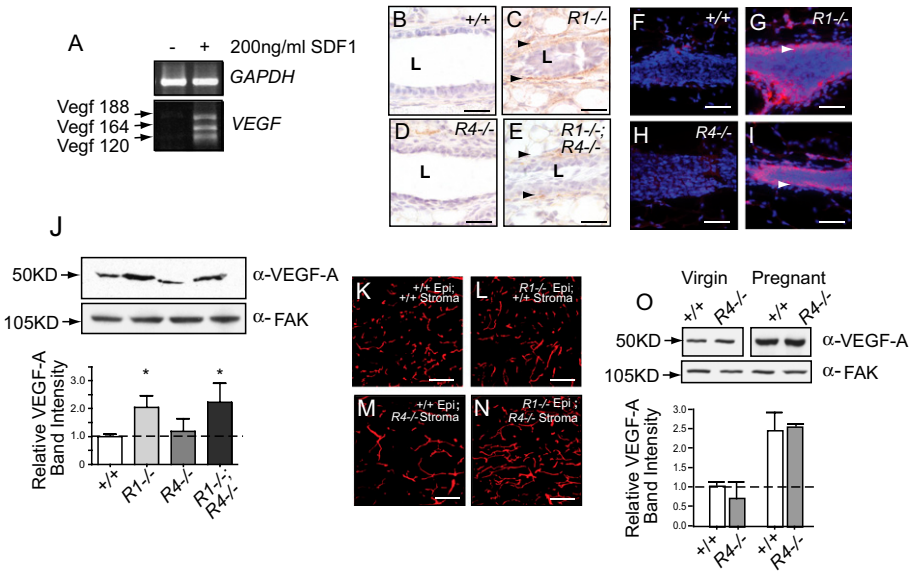

Fig. S3. The proangiogenic factor, VEGF, emanating from *Robo1*$^{-/-}$ and pregnant epithelium increases angiogenesis in *Robo4*$^{-/-}$ glands. (*A*) Treatment of primary mammary epithelial cells with SDF1 for 24 h leads to expression of all three isoforms of *Vegf-A* as assayed by RT-PCR. (*B–E*) SDF1 is expressed at higher levels in *Robo1*$^{-/-}$ and *Robo1*$^{-/-}$;*Robo4*$^{-/-}$ mammary epithelium. Representative images of immunostaining for SDF1 in $^{+/+}$ (*B*), *R1*$^{-/-}$ (C), *R4*$^{-/-}$ (*D*), and *R1*$^{-/-}$;*R4*$^{-/-}$ (*E*) mammary sections. Arrowheads indicate positive staining. Brown is DAB (3,3-diaminobenzidine) HRP reaction product from the secondary antibody. Blue is the hematoxylin counterstain. (Scale bar = 50 μm.) (*F–J*) VEGF-A is expressed at higher levels in *Robo1*$^{-/-}$ and *Robo1*$^{-/-}$;*Robo4*$^{-/-}$ mammary epithelium. Representative images of immunostaining for VEGF-A (red) in $^{+/+}$ (*F*), *Robo1*$^{-/-}$ (*G*), *Robo4*$^{-/-}$ (*H*), and *Robo1*$^{-/-}$;*Robo4*$^{-/-}$ (*I*) mammary sections. Blue is DAPI nuclei counterstain. Arrows indicate VEGF-A positive epithelium. (Scale bar = 50 μm.) (*J*) Representative immunoblots of anti-VEGF-A on mammary lysates (50 μg loaded; FAK immunoblot is loading control). Bar graph represent quantitative analysis of VEGF-A band intensity (ImageJ) (n = 3). Error bars = SEM, ***$P < 0.001$ unpaired t test. (*K* and *L*) Lack of *Robo1* in the epithelium does not alter blood vessel density in outgrowths. Representative images of mammary outgrowths, immunostained with anti-PECAM (red). (Scale bar, 50 μm.) (*M* and *N*) Increased blood vessel density with loss of *Robo1* in the epithelium combined with the loss of *Robo4*. Representative images of chimeric outgrowths immunostained with anti-PECAM (red). (Scale bar, 50 μm.) (*O*) VEGF-A levels increase twofold in pregnancy (day 12.5) with a similar increase occurring in both $^{+/+}$ and *Robo4*$^{-/-}$ glands. Equally loaded lysates (50 μg; FAK immunoblot is loading control) were probed with anti-VEGF-A (n = 3 per stage and per genotype). Representative blots are shown.

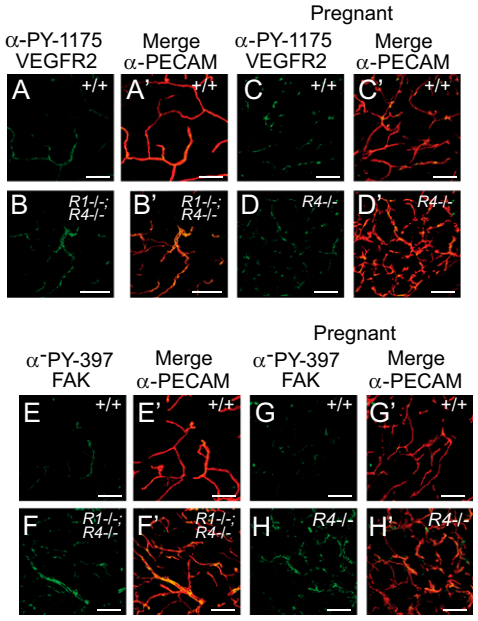

Fig. S4. ROBO4 functions to restrain VEGF/VEGFR2 signaling in the mammary gland. (*A–D*) Increased activation of VEGFR2 in *Robo1*$^{-/-}$;*Robo4*$^{-/-}$ adult glands and *Robo4*$^{-/-}$ pregnant (day 12.5) glands, compared to $^{+/+}$ controls. Representative images of immunostaining for PECAM (red) and P-Y1175 VEGFR2 (green) in mammary sections. (Scale bar = 50 μm.) (*E–H*) Increased activation of FAK in *Robo1*$^{-/-}$;*Robo4*$^{-/-}$ adult glands and *Robo4*$^{-/-}$ pregnant (day 12.5) glands, compared to $^{+/+}$ controls. Representative images of immunostaining for PECAM (red) and PY397-FAK (green) in mammary sections. (Scale bar, 50 μm.)

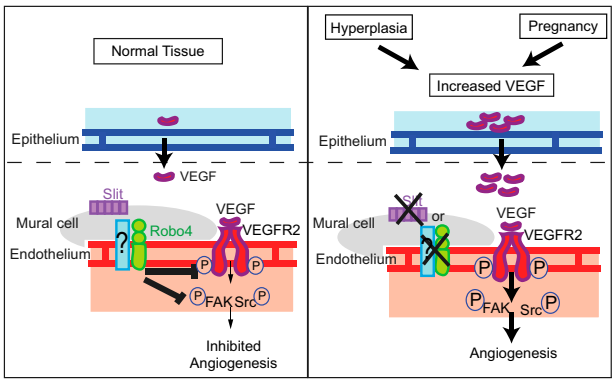

Fig. S5. ROBO4 functions in the endothelium as an inhibitor of angiogenesis. In normal tissue, SLIT is supplied by mural cells (gray oval) surrounding blood vessels (red). ROBO4 is involved in mediating the SLIT pathway, but there is likely an as yet unidentified coreceptor. The downstream consequence of SLIT signaling is to restrain angiogenesis by inhibiting the phosphorylation of VEGFR2 and downstream FAK and Src kinases. Conditions of hyperplasia (through loss of *Robo1* in the mammary epithelium) or pregnancy result in increased VEGF production in the epithelium (blue), but angiogenesis is still properly regulated in the presence of stromal SLITs or ROBO4. However, if *Slit* or *Robo4* expression is lost in the stromal compartment, then VEGF/VEGFR2 signals are no longer inhibited, leading to increased angiogenesis in response to the elevated levels of VEGF. The contribution of ROBO1 to the angiogenic phenotype is through its role in the epithelium as a negative regulator of SDF1 and VEGF expression.